Global Sensitivity Analysis of Environmental, Water Quality, Photoreactivity, and Engineering Design Parameters in Sunlight Inactivation of Viruses

Global sensitivity analysis of environmental, water quality, photoreactivity, and engineering design parameters in sunlight inactivation of viruses

Xinyi Zhang[a], Amanda Lardizabal[a], Andrea I. Silverman[b,c], Davide Vione[d], Tamar Kohn[e], Thanh H. Nguyen[a], Jeremy S. Guest[a,*]

Author Affiliations:

[a] Department of Civil and Environmental Engineering, University of Illinois at Urbana-Champaign, 205 N. Mathews Ave., Urbana, Illinois, 61801, USA

[b] Department of Civil and Urban Engineering, New York University Tandon School of Engineering, Brooklyn, New York, 11201, USA.

[c] School of Global Public Health, New York University, New York, New York, 10003, USA.

[d] Dipartimento di Chimica, Università degli Studi Torino, Via Pietro Giuria 5, 10125 Torino, Italy.

[e] Environmental Chemistry Laboratory, School of Architecture, Civil and Environmental Engineering (ENAC), École Polytechnique Fédérale de Lausanne (EPFL), CH-1015, Lausanne, Switzerland

***Corresponding author:** jsguest@illinois.edu, +1 (217) 244-9247

TOC Figure

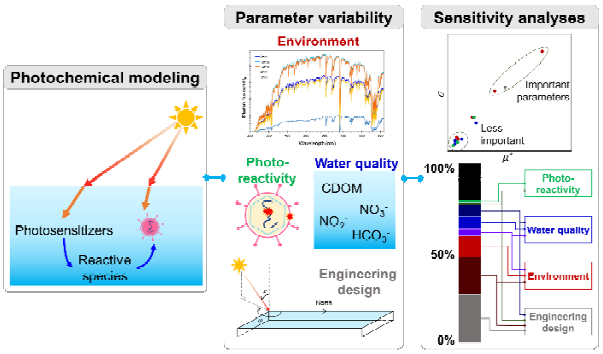

Abstract

Sunlight-mediated inactivation of microorganisms is a low-cost approach to disinfect drinking water and wastewater. The reactions involved are affected by a wide range of factors, and a lack of knowledge about their relative importance make it challenging to optimize treatment systems. To characterize the relative importance of environmental conditions, photoreactivity, water quality, and engineering design in the sunlight inactivation of viruses, we modeled the inactivation of three – human adenovirus and two bacteriophages – MS2 and phiX174 – in surface waters and waste stabilization ponds by integrating solar irradiance and aquatic photochemistry models under uncertainty. Through global sensitivity analyses, we quantitatively apportioned the variability of predicted sunlight inactivation rate constants to different factors. Most variance was associated with the variability in and interactions among time, location, non-purgeable organic carbon (NPOC) concentration, and pond depth. Photolysis quantum yield of the virus outweighed seasonal solar motion in the impact on inactivation rates. Further, comparison of simulated sunlight inactivation efficacy in maturation ponds under different design decisions showed reducing pond depth can increase the log inactivation at the cost of larger land area, but increasing hydraulic retention time by adding ponds-in-series yielded greater improvements in inactivation.

Keywords: solar inactivation, log removal, disinfection, uncertainty, APEX, SMARTS, lagoon

Introduction

Sunlight-mediated inactivation of bacteria and viruses has been widely studied in natural surface waters,[1–3] and has been leveraged as a low-cost approach to disinfection for drinking water (solar water disinfection, SODIS[4]) and wastewater (such as in waste stabilization ponds [WSPs][5] and constructed wetlands[6,7]). WSPs have gained popularity in recent decades, especially in developing communities and rural settings,[8,9] and have been promoted as strategy to mitigate human health risks caused by waterborne viruses. However, the efficacy of virus inactivation in these systems has been observed to be highly variable and often not optimized.[10] Virus removal in WSP systems has been reported to vary from 1-log to 4-log removal.[6] A number of factors contribute to inactivation variability within and across sites, including environmental conditions determining the incident sunlight irradiance, water constituents absorbing sunlight, and water depth affecting the level of sunlight attenuation. However, the relative importance of each factor, their interactions with each other, and the resulting implications for the design of optimized WSPs, have not been characterized.

Efforts have been made to characterize the individual factors that affect disinfection within solar-driven treatment systems.[11] The effects of a wide range of variables on sunlight disinfection rates have been investigated. These variables include water matrix characteristics (e.g., pH,[12–14] dissolved oxygen [DO] concentration,[12,14] salinity,[15] the concentration and type of natural organic matter,[13,16,17] the presence of other light absorbing water constituents,[12,18] temperature[12,17,19]), water depth,[7,20] sunlight irradiation spectrum,[21,22] and virus charateristics.[1,10,21] The results have been used by researchers to develop semi-mechanistic model equations that describe the sunlight inactivation rate constants of viruses as a function of the most influential inputs.[7,22–25] These equations have been able to predict inactivation rates in good agreement with measurements in a few experimental settings but are yet to be examined across wide ranges of spatial-temporal locations or physiochemical conditions of water.[7,24–26]

Existing sunlight inactivation rate models for viruses assume first-order inactivation kinetics and estimate decay rates as a sum of the endogenous and exogenous inactivation rate constants.[11] Endogenous inactivation is caused by damage to viruses resulting from direct absorption of photons by the virion. Therefore, most inactivation rate models are based on biological weighting functions (also known as photoaction spectra), which describe the wavelength-dependent sensitivity of viruses to endogenous sunlight damage,[22,26,27] although different approaches take into account the separate effects of virion absorption and photon action.[23,24] Exogenous inactivation, on the other hand, results from damage by exogenous photo-produced reactive intermediates (PPRIs) – formed by external photosensitizers upon their absorption of sunlight photons – and can be described by second-order reaction kinetics as a function of steady-state PPRI concentrations[18]. Singlet oxygen ($^1O_2$) has been found to be the most important PPRI contributing to exogenous inactivation of the MS2 bacteriophage,[3,7,13,21,25] which was considered suitable as surrogate for monitoring virus reduction in wastewater reclamation.[28] Some studies have modeled exogenous inactivation rates as a function of steady-state concentration of $^1O_2$ alone,[7,25] while others have also included the triplet-state chromophoric dissolved organic matter ($^3CDOM^*$), hydroxyl radical ($^\bullet OH$), and carbonate radical ($CO_3^{\bullet-}$) in the modeling of exogenous decay rate.[23,24] The latter adapted a series of previously-developed equations for aqueous photochemical reactions[29–32] and experimentally derived the photoreactivity parameters for several virus species.[23–25] Despite progress in the quantification of individual parameters and relationships driving sunlight inactivation of viruses, a systematic comparison to determine the relative importance of virus-specific parameters and their interactions with other scenario-specific factors (e.g., location, treatment system design) is still missing.

The objective of this work was to elucidate the environmental, water quality, photoreactivity, and engineering design parameters governing the efficacy and variability of

sunlight virus inactivation to reduce the uncertainty of model predictions and support the design of more reliable sunlight-driven disinfection systems. The variability of nine parameters of environmental conditions, water quality, and engineering design, and the uncertainty of five viral photoreactivity parameters were characterized based on existing knowledge and experimental data. Given the susceptibility to endogenous and exogenous inactivation and the general resistance to sunlight irradiation differ among virus species,[1,10,28] we ran Monte Carlo simulations of the integrated model by simultaneously varying the parameters for one human enteric virus and two bacteriophages (surrogates for enteric viruses) across two types of water (natural surface water, WSP water). Simulation output k_{total} (the first-order rate constant of virus inactivation) was used to compare the relative importance of the fifteen parameters and quantify the interactions among them through robust global sensitivity analyses (i.e., the Morris One-at-A-Time screening technique and subsequently Sobol's variance-based sensitivity indices). Finally, to illustrate the influence of pond design on virus inactivation performance, we predicted the disinfection of bacteriophage MS2 in a maturation pond system with different designs by modeling continuous stirred-tank reactors (CSTRs) in series.

Methods

Photochemical modeling of sunlight virus inactivation. Sunlight inactivation rate constants were modeled for three viruses: human adenovirus (dsDNA), and bacteriophages MS2 (ssRNA) and phiX174 (ssDNA). The sunlight inactivation rate through a well-mixed water column k_{total} was modeled as the sum of two mechanisms – endogenous and exogenous – following the photochemical model and the algorithm used by the APEX software.[29] Adenovirus and MS2 are among the most resistant viruses to UV disinfection, while phiX174 exhibits the opposite relative susceptibilities to endogenous and exogenous inactivation.[11]

$$k_{total} = k_{endo} + k_{exo} \quad (1)$$

k_{endo}, in h^{-1}, was predicted as the first-order reaction rate constant of the direct photoinactivation of the virion. k_{exo} [h^{-1}], on the other hand, was predicted as the pseudo first-order rate constant of a series of parallel photooxidation reactions between the virion and exogenous PPRIs ($^1O_2$, $^{\bullet}OH$, $CO_3^{\bullet-}$, and $^3CDOM^*$).

$$k_{endo} = \int_{\lambda = 280\ \text{nm}}^{710\ \text{nm}} \Phi_{virus}\varepsilon_{virus}(\lambda) \cdot p^0(\lambda) \cdot \frac{1 - 10^{-\alpha(\lambda)l}}{\alpha(\lambda)l} d\lambda \quad (2)$$

$$k_{exo} = \sum_{PPRI} k_{virus,PPRI}[PPRI]_{ss} \quad (3)$$

k_{endo} depends on the susceptibility of virion to sunlight inactivation (Φ_{virus}, ε_{virus}) and the virion's exposure to sunlight in the water ($p^0(\lambda)$, $\alpha(\lambda)$, l), as shown in eq. (2). ~~$\Phi_{virus}\varepsilon_{virus}$~~A virion's exposure to sunlight in water depends simultaneously on the incident sunlight irradiance and the attenuation by water constituents as sunlight transmits through the water body. $\alpha(\lambda)$ [cm^{-1}], the specific water absorbance over a 1-cm optical path, was predicted as an exponential function of the concentration of non-purgeable organic carbon (NPOC, in mg-C·L^{-1}) and wavelength:[29]

$$\alpha(\lambda) = A \cdot [NPOC] \cdot e^{-B\lambda} \quad (4)$$

k_{exo} (eq. (3)) depends on the viral susceptibilities to PPRIs ($k_{virus,PPRI}$) and the steady-state concentrations of these PPRIs ($[PPRI]_{ss}$) that are determined by the steady-state conditions that encompass formations sensitized by CDOM, nitrate, and nitrite upon sunlight absorption and loss through scavenging reactions with water constituents (e.g., DOM, inorganic carbon, O_2), or simply energy loss.[29] So, the APEX model predicts $[PPRI]_{ss}$ as functions of water chemistry, water depth, and incident sunlight spectrum.[29] All viral photoreactivity parameters for adenovirus, MS2, and phiX174, including quantum yield Φ_{virus} [mol virus inactivated · (mol

photon absorbed)$^{-1}$], molar absorption coefficient ε_{virus} [(mol virus)$^{-1}$·L·cm^{-1}], and second-order reaction rate constants $k_{virus,PPRI}$ [L·(mol virus)$^{-1}$·s^{-1}], have been estimated in previous studies using the observed inactivation rates in controlled experiments.[23,27]

Since k_{total} is an average value over the well-mixed water column, the model considered sunlight penetration and attenuation through a water body by including the optical path length, l [cm], in the prediction of k_{endo} and $[PPRI]_{ss}$, assuming Lambert-Beer's Law. l is derived from the depth, d [cm], of the well-mixed water column and the zenith angle, z [°], of the sunlight incident on the water surface.[33]

$$l = \frac{d}{\sqrt{1 - \left(\frac{\sin z}{1.34}\right)^2}} \tag{5}$$

$p^0(\lambda)$ [Einstein·cm^{-2}·s^{-1}·nm^{-1}], the photon flux density of the incident sunlight, was used to model both k_{endo} and $[PPRI]_{ss}$. As important inputs to the photochemical model, $p^0(\lambda)$ and z were modeled by the SMARTS program (Simple Model of the Atmospheric Radiative Transfer of Sunshine, version 2.9.5) as a function of environmental conditions.[34] To automate simulation of k_{total} under varying sunlight conditions, the APEX model and the SMARTS program were connected and run through Python.

Variability of input parameters. To identify the influential factors responsible for variability in the sunlight inactivation rates of viruses, this work compared the relative importance of fourteen parameters in the sunlight inactivation model (Table S3), which characterize environmental conditions, virus photoreactivity, water quality, and engineering design of the reaction system. Geographic location, elevation, and seasonal and diurnal motions of the sun affect the sunlight inactivation rate by determining the solar position and, subsequently, the sunlight incident on water surface. Therefore, in the modeling of $p^0(\lambda)$ and z,

we considered the variability of latitude, longitude and elevation of geographical locations exposed to perennial sunlight, i.e., between 60° S and 60° N. Values of these parameters were sampled from the Shuttle Radar Topography Mission (SRTM) elevation data (1-km resolution) to represent the empirical distribution.[35] The influence of seasonal and diurnal motions of the sun was captured by running simulations on the 22nd day of each month across twelve months, and between the sunrise and sunset times specific to the location and the date. Other parameters in the SMARTS program either were assumed constant (in which case the default values provided by SMARTS were used) or were estimated as functions of the geographic and temporal parameters (Tables S1, S2).

Uncertainties have been reported around measurements of most parameters characterizing viral photoreactivity in existing studies (Table S3).[23,24] Estimations of Φ_{MS2} from two different studies differed by an order of magnitude.[23,27] To investigate to what degree such uncertainty around Φ_{virus} would affect the prediction of k_{total}, we assumed a uniform distribution within 10~100% of the values reported by Mattle et al.[23] As for $k_{MS2,^1O_2}$, the lower (1.2×10^8 $M^{-1}\cdot s^{-1}$) and upper (1.97×10^9 $M^{-1}\cdot s^{-1}$) bounds were estimated from the experimental data reported by Silverman et al.[21] and Rosado-Lausell et al.[18] respectively, based on the observed correlations between k_{obs} of MS2 and $[^1O_2]_{ss}$. Several values within this range were also obtained in other studies.[3,13]

Analyses were conducted for two water typologies with different water quality – one more typical of a natural surface water and one more typical of a WSP. According to the sources of water chemistry parameters in the model, the natural water was defined as lake water.[36–38] The WSP was defined as the WSP in Vuiteboeuf, Switzerland.[24]

CDOM, nitrate, and nitrite are important photosensitizers for the formation of PPRI.[11,29] As the main sunlight absorber in natural surface water and WSP water,[5,24,29] CDOM, which can

be estimated from DOC (dissolved organic carbon) or NPOC concentrations (eq. (4)), is highly variable in different water bodies. Low levels, such as 0.54±0.03 mg·L^{-1} NPOC, have been observed in lake water.[39] Other studies suggested freshwater lakes can have up to 60 mg·L^{-1} DOC[16] and, on average, DOC ≈ 1.33 NPOC.[39] Concentrations between these values have been measured in a variety of waters (WSP, treatment wetland, clear coastal water, rivers, lakes).[2,7,19,23,24,40] Therefore, a uniform distribution within [1, 40] mg-C·L^{-1} was assumed for the concentration of NPOC in this study. Similarly, a wide range of nitrate concentrations in natural surface waters have been reported, ranging from 0.7 mg·L^{-1} for the intake water to the Wilson water treatment plant (Durham NC, USA)[40] to about 61 mg·L^{-1} from the upper River Derwent (due to agricultural land use in the vicinity of the catchment).[41] Nitrite concentrations are usually low in natural surface water (<0.1 mg-N·L^{-1}) and WSP water (1.2×10^{-5} M)[23,24]. Regulations on the maximum nitrite concentration during wastewater treatment processes in Switzerland is 0.3 mg-N·L^{-1}.[42]So, we assumed uniform distributions within [1.13×10^{-5}, 9.84×10^{-4}] mol·L^{-1} and [0, 3.57×10^{-5}] mol·L^{-1} for nitrate and nitrite in simulations, respectively. To account for the variability in the absorbance spectra of natural surface water and WSP water, uniform distributions within the confidence intervals (Table S3) were assumed for the parameters A and B in eq. (4).[24,37]

Water depth is a key design parameter in the model equations, as it determines the optical path length and sunlight attenuation. The depth of a typical maturation pond for disinfection is usually 0.8~1.5m.[9,20,43–45] 0.4 m is often considered a minimum depth in practice, and ponds deeper than 1.8 m are rarely dedicated for disinfection.[46] Therefore, a uniform distribution in [0.2, 2] m was assigned to water depth in simulations.

Uncertainty analysis. Uncertainty analysis of the sunlight inactivation model allowed quantifying the variability in k_{total} due to the simultaneous variations of fourteen input parameters. Assuming the input parameters are independent of each other, we generated

100,000 Latin-hypercube samples from the 14 parameter distributions (Table S3) for each virus-water combination and propagated the parameter variabilities through Monte Carlo simulations of the sunlight virus inactivation model.

Global sensitivity analysis. Sensitivity analysis (SA) of the sunlight inactivation model allowed evaluation of how the uncertainty in k_{total} can be apportioned to variabilities in each of the parameters. Compared to local methods (i.e., evaluating the impact of each parameter individually), results of global SA are more robust and can reveal how one parameter can affect the impact of another parameter on k_{total} because samples are generated across the entire parameter space. The Morris one-at-a-time screening technique was first used in this study to rank the parameters according to their influences on the value of k_{total}.[47] Morris method produces two sensitivity indices μ^* and σ. Index μ^* of a parameter indicates its overall influence on k_{total} across its range of variation, while σ detects whether it is interacting with other input parameters to influence k_{total} (e.g., the variability in k_{total} caused by the fluctuation of NPOC concentration depends on pond depth).[48,49] A larger σ of a parameter implies stronger interactions between this parameter and other parameters. The ratio σ/μ^* is an indicator of linearity and monotonicity of the model. With most σ/μ^* greater than 1, one can conclude the model is non-linear and/or non-monotonic. 17,000 simulations were performed to calculate μ^* and σ for each combination of virus species and water type, following an economical sampling technique designed by Morris.[47,50]

Sobol's variance-based sensitivity analysis was performed to quantitatively attribute the variance of k_{total} to the uncertainties or variabilities of different input parameters (Table S3). Sobol's method offers three sensitivity indices: the main effect S_i, the second-order interaction effect S_{im}, and the total effect S_{Ti}. For a parameter X_i, S_i indicates the proportion of output

uncertainty removed by fixing X_i. S_{im} equals to the proportion of output variance caused by interaction between X_i and X_m. S_{Ti} is the proportion of output uncertainty associated with X_i's variability and all its interactions with other parameters in the model. It can be interpreted as the expected output variance when only X_i is left undetermined.[51,52] In this study, 300,000 simulations were performed for each combination of virus species and water type to estimate S_i, S_{im}, and S_{Ti} of the 14 parameters with acceptable uncertainty.[51,53] Python module SALib was used for the execution of sampling and computation of sensitivity indices[54].

Modeling of MS2 inactivation of a maturation pond. To investigate the influence of engineering design on the virus disinfection efficacy of a typical WSP system, sunlight inactivation of MS2 in a fictitious maturation pond located at 90°W, 42°N over 24-hour cycles during the summer solstice (June 22nd) and the winter solstice (Dec. 22nd) was simulated by coupling the sunlight virus inactivation model with a 3-D CSTR model (details of the model are provided in the SI). MS2 was chosen because it had been most thoroughly investigated as a reference organism in existing studies of sunlight virus inactivation. Pair-wise comparisons of MS2 log10 removal by sunlight inactivation were performed to illustrate the impact and the cost of individual design decisions on hydraulic retention time (HRT), system configuration, pond depth, and pond length-to-width ratio under uncertainties of the photoreactivity and water quality parameters (Table S3).

Results and Discussion

Simulated inactivation rates. Considerable variability of simulated k_{total} was observed due to simultaneous variation of the 14 parameters. Simulated k_{total} had a right-tail distribution across a wide range for all three viruses, and the maximal simulated k_{total} were 24~56 times greater than the mean values, depending on the virus species and the water type (Figure 1). In natural water, the middle 50% of simulated k_{total} ranged from 0.005 h^{-1} to 0.05 h^{-1} for adenovirus and from 0.01 h^{-1} to 0.09 h^{-1} for MS2. In WSP water, the middle 50% of simulated k_{total} ranged in 0.01~0.08 h^{-1} for adenovirus and in 0.03~0.19 h^{-1} for MS2. The greatest variability in simulated k_{total} was observed in phiX174 inactivation, whose coefficient of variation was 3.33 in natural water and 2.20 in WSP water (Table S6). Its middle 50% fell in 0.02~0.29 h^{-1} and 0.02~0.38 h^{-1} in natural water and WSP water, respectively. The greater variability of phiX174's k_{total} was largely attributed to the greater contribution of endogenous inactivation in relation to other mechanisms. When all parameters were varied simultaneously, inactivation rates by $CO_3^{\bullet-}$, direct photolysis (i.e., endogenous mechanism), and $^{\bullet}OH$ had the greatest variabilities (measured by the coefficient of variation) among all mechanisms, but neither $CO_3^{\bullet-}$ nor $^{\bullet}OH$ dominated inactivation (< 20% k_{total} in most cases) for any of the three viruses. Therefore, the virus with higher relative susceptibility to endogenous inactivation is subject to greater variability in the overall inactivation rate when environment and water conditions change.

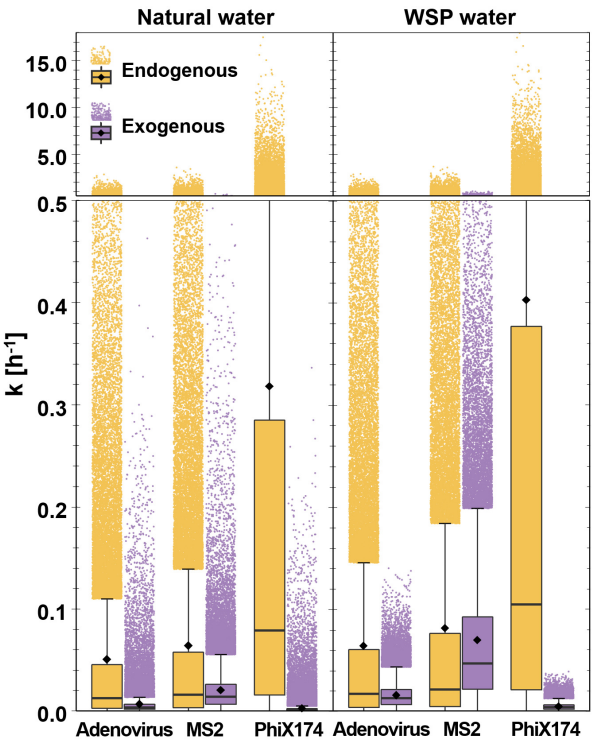

Figure 1. Simulated k_{endo} and k_{exo}. The box indicates 1st, 2nd and 3rd quartiles. The lower whisker shows the minimum, and the upper whisker = 3rd quartile + 1.5×interquartile range. Mean values are indicated by the diamonds (♦). Outliers were spread out horizontally for better visualization.

While simulation results generally agreed with current estimation or measurements of the sunlight inactivation of MS2 and phiX174[1,23,24], simulations across the parameter space were able to reveal different trends of inactivation rates under extreme conditions. Given greater photochemical reactivity of ssDNA compared to ssRNA, phiX174 is expected to have higher k_{total} than MS2. However, in approximately 27% of all simulated cases, which had relatively larger zenith angle, higher latitude, higher NPOC concentration, higher water absorbance of long wavelengths and were at a time further away from noon ($p < 2.2\times10^{-16}$; Table S8), phiX174

had lower k_{total} than MS2 under identical environmental conditions, water quality, and water depth (Fig S8). It means MS2 inactivation was less negatively impacted by the conditions that are unfavorable to endogenous mechanism, because MS2 is more susceptible to reaction with PPRIs than phiX174. Indeed, PPRIs can be formed by light at wavelengths greater than 320 nm that can penetrate deeper into the water column, while nucleic acids and capsid proteins – chromophores in endogenous virus inactivation – have minimal absorption beyond 320 nm.[55]

Similar to the model prediction by Mattle et al.,[23] adenovirus constantly had lower k_{total} than MS2 in simulation regardless of water quality or environmental conditions (Fig S8). Yet some studies have found adenovirus and MS2 to have similar resistance to sunlight inactivation in clear water and some natural waters,[1,21,56]. while others have observed adenovirus to be more susceptible to sunlight inactivation than MS2 in WSP water and other natural waters[21,23,56].

Under identical environmental and water conditions, sunlight inactivation in WSP water was estimated to be faster than in natural water for all three virus species in most cases (Table S9, Fig S9), mainly because the absorbance spectra of the simulated WSP water tended to be more favorable for both direct photolysis and inactivation by $^1O_2$. Values of A and B in eq. (4) determined that the simulated WSP water should have higher absorbance of visible light than natural water given the same NPOC concentration, which tends to increase $[^1O_2]_{ss}$ and thus k_{exo}. On the contrary, natural water was predicted to have higher absorbance of UV light, resulting in fewer UV photons available to cause endogenous sunlight inactivation. This effect increases with the depth of water column and creates larger difference between inactivation rates in WSP water and natural water.

The influence of water quality on inactivation by reactive species. Consistent to previous estimation,[23] direct photolysis had greater contribution to phiX174 inactivation than any reactive species in almost all cases, accounting for 60~100% of k_{total} across different

environmental and water conditions. For adenovirus, contribution of direct photolysis to k_{total} varied across a wider range but was mostly greater than 40%. Silverman et al. measured the contribution by UVB irradiation to range from 85% to 96% in five coastal water samples.[21] In WSP water, $^1O_2$ and $^3CDOM^*$ became a greater contributor to phiX174's k_{total} than direct photolysis in a small number of cases, which tended to be at a time close to sunrise or sunset (Fig S11) and have high NPOC concentration (> 30 mg-C·L^{-1}). The greatest variation of relative contribution by different mechanisms was observed for MS2 inactivation, especially in natural water (Figure 2). Different studies also reported very different measurements or estimations of the share of k_{endo} for MS2. Love et al. measured 13% in seawater.[1] The model estimation by Silverman et al. was roughly 86% in treatment wetlands.[7] Mattle et al. estimated the contribution of exogenous inactivation to be 41%,[23] and the estimation by Kohn et al. suggested 20~56% depending on water depth.[24]

Figure 2 showed a strong correlation between NPOC concentration and the relative contributions of PPRIs to exogenous inactivation. A significantly positive sample Pearson correlation coefficient ($r = 0.69$, $p < 2.2\times10^{-16}$) was estimated between NPOC concentration and the share of $^1O_2$ and $^3CDOM^*$. Unlike $^3CDOM^*$ or $^1O_2$, which are produced by CDOM as the dominant photosensitizer, $^\bullet OH$ can also be produced from NO_3^- and NO_2^-; both $^\bullet OH$ itself and $^3CDOM^*$ can sensitize the formation of $CO_3^{\bullet-}$. When NPOC concentration was below 5 mg-C·L^{-1}, the formation of $^3CDOM^*$ and $^1O_2$ became limited, while the formation of $^\bullet OH$ and $CO_3^{\bullet-}$ could still be sensitized by NO_3^- and NO_2^-. Moreover, at low NPOC there is limited scavenging of $^\bullet OH$ and $CO_3^{\bullet-}$ by DOM.[37] This suggests $^1O_2$ is not always the most important PPRI for the exogenous inactivation. More specifically, 16% of the simulated cases had higher inactivation rates by $^\bullet OH$ and $CO_3^{\bullet-}$ than that by $^3CDOM^*$ and $^1O_2$ (Table S10).

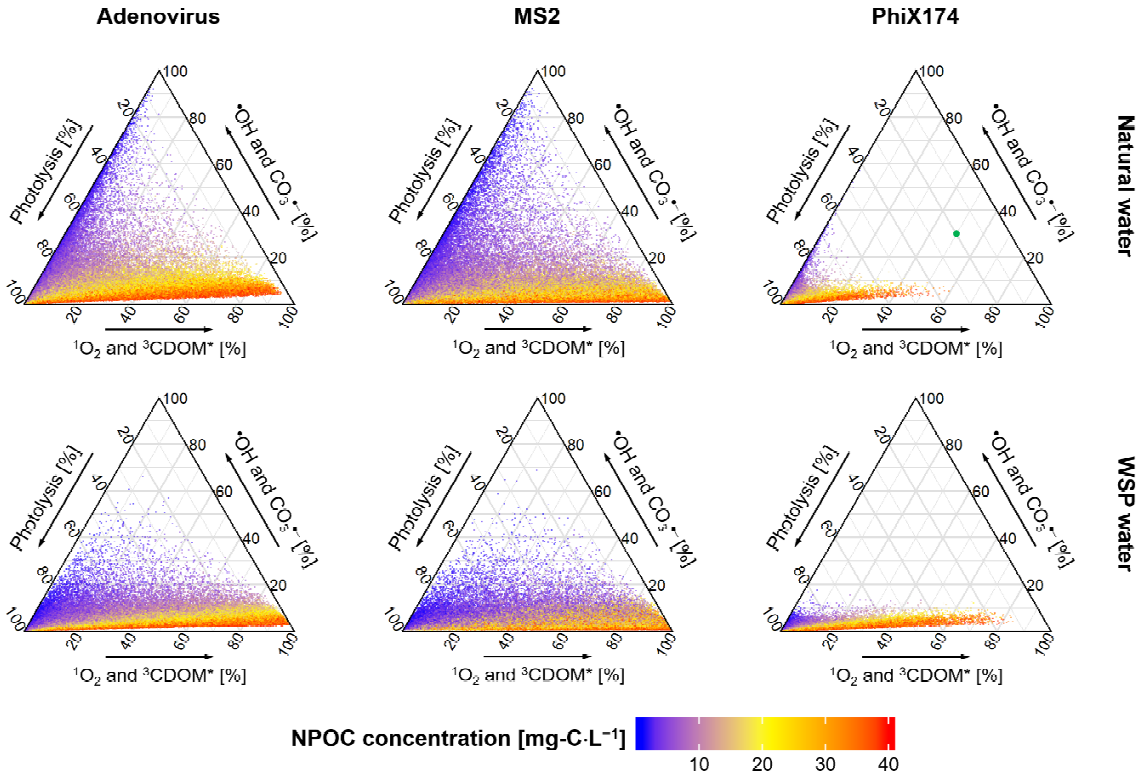

Figure 2. Ternary plot of contributions of inactivation by different mechanisms ("Photolysis [%]" refers to endogenous inactivation) vs. NPOC concentration in simulation. For example, the green dot in the top-right ternary plot indicates that 50% of k_{total} is contributed by $^3CDOM^*$ and $^1O_2$, 30% by $^\bullet OH$ and $CO_3^{\bullet-}$, and 20% by direct photolysis. $^3CDOM^*$ and $^1O_2$ were grouped as reactive species whose formation is dominantly sensitized by CDOM. $^\bullet OH$ and $CO_3^{\bullet-}$ were grouped, for their formation can also be sensitized, directly or indirectly, by NO_3^- and NO_2^- besides CDOM. Moreover, both radicals are efficiently scavenged by DOM.

The linear correlation often observed between the apparent MS2 inactivation rate constant and $[^1O_2]_{ss}$ in previous studies[3,13,18] did not hold across the various environmental

conditions or water matrix in simulations. In cases where $^{\bullet}OH$ and $CO_3^{\bullet-}$ outweighed $^3CDOM^*$ and $^1O_2$, the simulated water had significantly lower [NPOC], higher [NO_3^-] and [NO_2^-], as well as lower absorbance of sunlight at long wavelengths ($p < 2.2\times10^{-16}$). This can be explained by the difference in the absorption spectra of the photosensitizers – UVA and visible lights can be absorbed by CDOM but barely by NO_3^- or NO_2^-.[55]

Relative importance of environmental, photoreactivity, water quality, and engineering design parameters to k_{total}. Among the 16 parameters (location was analyzed as three independent variables – latitude, longitude, and altitude), time of the day was ranked the most influential parameter (measured by μ^*) in the Morris analysisk_{total} (Figure 3), followed by latitude. They determined the spectral irradiance and the zenith angle of incident sunlight, which greatly impact endogenous inactivation. They also had the largest σ among all parameters, meaning they had the strongest interactions with other parameters. For example, the change in k_{total} resulting from the reduction of NPOC concentration depends on the location of the water body and the local time. Depth of the water column, NPOC concentration, and quantum yield Φ_{virus} were the next most important parameters to k_{total}, with similar values of μ^* and σ. Water depth determined the length of the optical path and thereby the attenuation of sunlight. CDOM, as the major photosensitizer in water that occurs in higher amounts at high NPOC,[29] affects not only the steady-state concentrations of reactive species k_{exo}but also k_{endo} through competition with virion in absorbing sunlight photons.

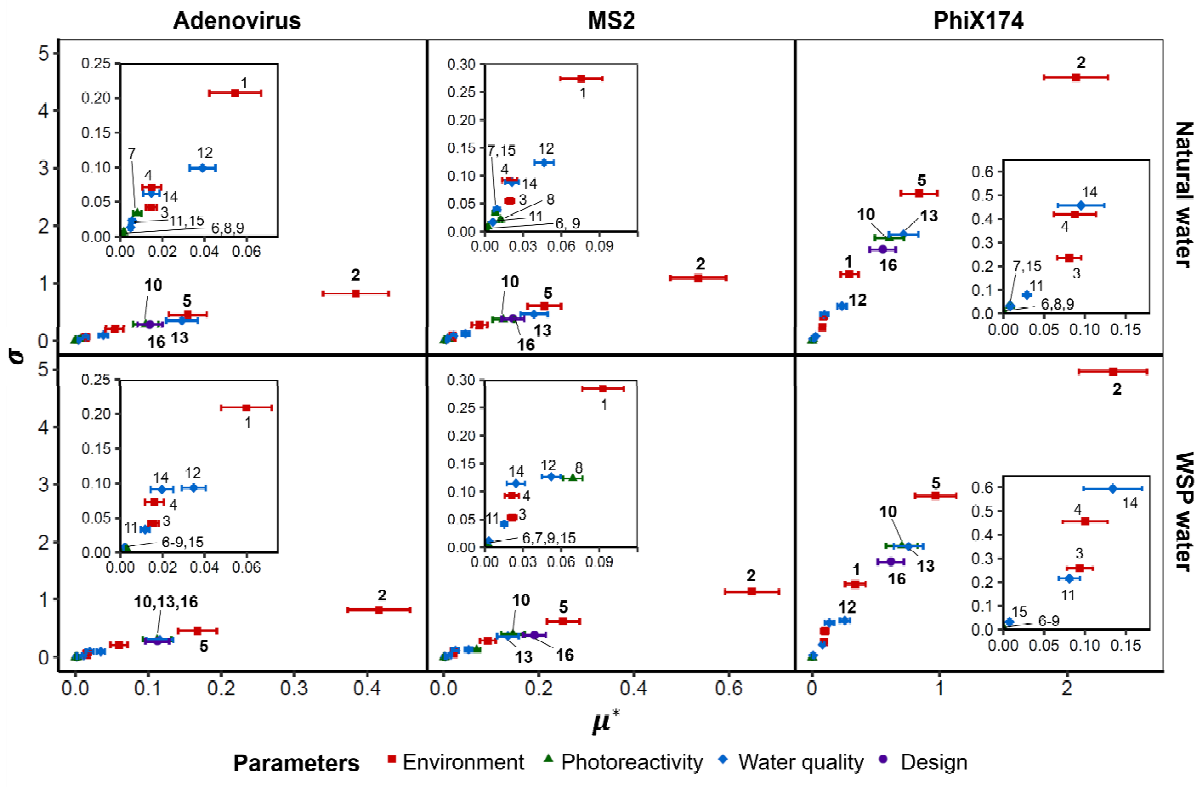

Figure 3. Morris sensitivity indices of k_{total} against 16 parameters: 1 – month, 2 – time, 3 – altitude, 4 – longitude, 5 – latitude; 6 – $k_{virus,\ ^{\cdot}OH}$, 7 – $k_{virus,\ CO_3^{\cdot-}}$, 8 – $k_{virus,^1O_2}$, 9 – $k_{virus,^3CDOM^*}$, 10 – Φ_{virus}; 11 – A, 12 – B, 13 – [NPOC], 14 – [NO_3^-], 15 – [NO_2^-]; 16 – water depth. Whiskers indicate the 95% confidence intervals of μ^*.

Seasonal motion of the sun, as indicated by "month", was outweighed by the viral susceptibility to direct photolysis Φ_{virus} in prediction of k_{total}. This is largely attributed to the considerable uncertainty of Φ_{virus} around its "true" value in simulations. Estimation of Φ_{virus} have been a challenging task limited by the accuracy of radiometers in measuring light output over the UVB range, which are the most relevant wavelengths for endogenous inactivation. Different radiometers yielded estimations of Φ_{virus} that differed by an order of magnitude.[23,27]

Therefore, using an estimated Φ_{virus} in modeling without an irradiance spectrum measured by the corresponding radiometer would likely lead to biased prediction. The inactivation rate constant of MS2 by $^1O_2$ was also among the influential parameters, since MS2 is relatively susceptible to exogenous inactivation and the uncertainty around $k_{MS2,^1O_2}$ was greater than other inactivation rate constants. Other environmental parameters (longitude and altitude), water quality parameters (A, B, [NO_3^-] and [NO_2^-]) and most virus photoreactivity parameters had relatively small impacts on k_{total}.

The σ/μ^* ratios of all parameters varied in the model were greater than 1, implying nonlinear and/or nonmonotonic effects of different parameters on k_{total}. For example, the marginal improvement in k_{total} by reducing water depth is greater at 0.2 m than at 1.2 m, since sunlight, especially at short wavelengths, attenuates drastically at the first 20 cm of the optical path. Increasing latitude from the south to the north hemisphere would firstly increase and then decrease k_{total}, which most local SA methods would fail to detect. The non-linearity and non-monotonicity of the model makes Sobol's method a valid choice for the quantification of relative importance of parameters in the model, because it does not rely on any assumption of the model structure.

In general, results of Morris and Sobol's analyses agreed well with each other. Despite the difference in the relative susceptibilities to sunlight inactivation mechanisms among different virus species, the largest values of main effect S_i were invariably obtained for time of the day (12.8~24.4%), NPOC concentration (4.5~15.9%), and water depth (8.0~14.4%), meaning these parameters are the most important sources of variance in k_{total} regardless of virus species or water type (Figure 4). Second to them were location and quantum yield Φ_{virus}, whose main effects were 4.0~4.9% and 3.0~4.3%, respectively. It implies that eliminating the uncertainty of

Φ_{virus} can reduce the variance of k_{total} by at least 3.0%. The importance of location was less significant in Sobol's analysis than in Morris analysis. However, we believe the result of Sobol's analysis was more accurate, since location was sampled from empirical land-area elevation dataset. Specific to MS2 inactivation in WSP water, the uncertainty of $k_{virus,^1O_2}$ alone accounted for 2.4% of the variance of k_{total}. $\sum_i S_i$ was approximately 55% for MS2 in WSP water and less than 50% for other virus-water combinations, i.e., approximately half of the variance of k_{total} was contributed by interaction among parameters. Therefore, examining each factor individually would likely lead to underestimation of its impact on the sunlight inactivation rates.

Parameters with large main effects to k_{total} tended to also have strong interaction effects between each other (Figure 4). About 15~23% of the variance of k_{total} were caused by the interactions between the top 6 pairs of parameters among time of the day, water depth, NPOC concentration, location, and Φ_{virus}. Although 70% of the variance in k_{total} prediction can be attributed to only five parameters, the variability in these parameters (e.g., variability in local time due to diurnal motion of the sun, fluctuation of NPOC concentration in water) cannot always be reduced or eliminated, i.e., a proportion of k_{total} variance is inevitable. Therefore, the uncertainty in most photoreactivity parameters and water quality parameters would most likely stay uninfluential to the k_{total} of a treatment system within the range evaluated. Total effect S_{Ti} is a valid indicator of how much variation in k_{total} is expected if one cannot reduce the variability of a single parameter. For example, if the uncertainty in Φ_{virus} and $k_{MS2,^1O_2}$ had been greatly reduced, and the concentrations of photosensitizers remained constant, the prediction of k_{total} between sunrise and sunset on a certain day for a certain treatment system would still be subject to approximately 50% of the total variance, given the S_{Ti} of "hour" was 46.9~52.5% (Table S11).

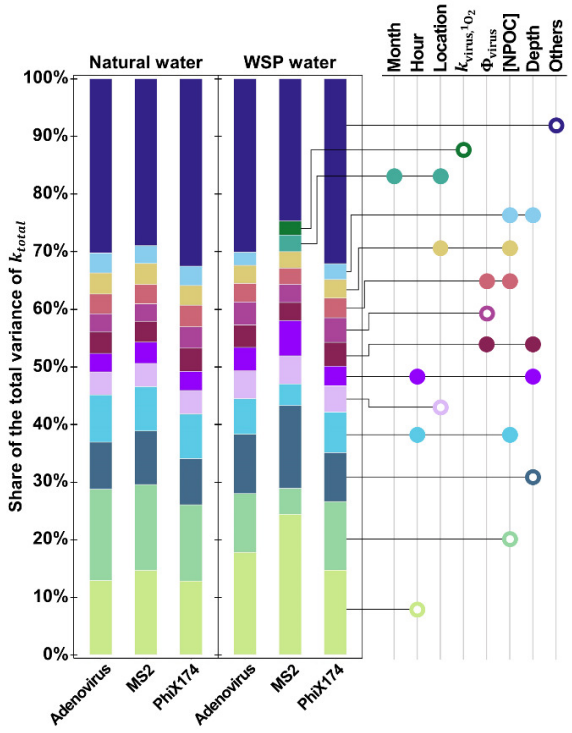

Figure 4. Decomposition of the variance of k_{total} into variances introduced by different parameters. Filled dots represent interaction effects (S_{im}) between two parameters. Hollow dots indicate main effects (S_i) of individual parameters. Only sensitivity indices larger than 2% are presented. Other parameters include $k_{virus,\cdot OH}$, $k_{virus,\ CO_3^{\cdot-}}$, $k_{virus,^3CDOM^*}$, A, B, [NO_3^-] and [NO_2^-].

The impact of individual maturation pond design decisions on disinfection efficacy. Among the most influential parameters identified above, water depth can be fixed and optimized in treatment system design. Starting from a 1.5 m-deep maturation system operating at HRT = 5 days, reducing its pond depth to 0.5 m was estimated to improve the inactivation efficacy on average by 0.7 log during the summer solstice and by 0.4 log during the winter solstice (Figure 5). However, to maintain its treatment capacity (i.e., constant influent flow rate), it required a 200% increase in pond area. In comparison, increasing the HRT to 9 days by

adding 4 identical 1.5 m-deep ponds to the system was estimated to yield greater improvements in log inactivation in both summer (1 log) and winter (0.4 log), while required pond area only increased by 80%. Therefore, adding ponds to increase HRT is a more cost-effective design decision than reducing pond depth within the range evaluated. Figure 5 also showed both required pond area and improvement in log inactivation increased linearly with HRT, while reducing depth had increasing marginal improvement in log inactivation. That is to say, further reduction of pond depth may yield equal or higher improvement than increasing HRT, albeit with even larger required pond area. It should also be noted each pond was assumed to be an ideal CSTR, which may not model an actual treatment system where stratification can occur in deep ponds.

Provided sunlight inactivation of viruses follows first-order kinetics, increasing the number of ponds in series while fixing HRT was expected to improve the inactivation efficacy of the system, assuming the water quality parameters were not affected (Fig S12). However, improvement of log inactivation by changing the pond configuration would still be negligible in winter when the incident spectral irradiance is the main limiting factor to inactivation. Besides, a less-mix system may experience greater diurnal fluctuations of effluent virus concentration due to the absence of sunlight inactivation during the night, if the HRT is not long enough. Although length-to-width ratio of the maturation pond had negligible impact on the inactivation efficacy of the system in simulations (Fig S13), it may affect the hydraulic efficiency and the level of mixing in an actual system.

Seasonal motion of the sun and the uncertainty in water quality still induced high uncertainty in the prediction of log inactivation regardless of design decisions, which should be fully considered in the engineering design of treatment systems relying on sunlight inactivation for disinfection for safe discharge or reuse of effluents.

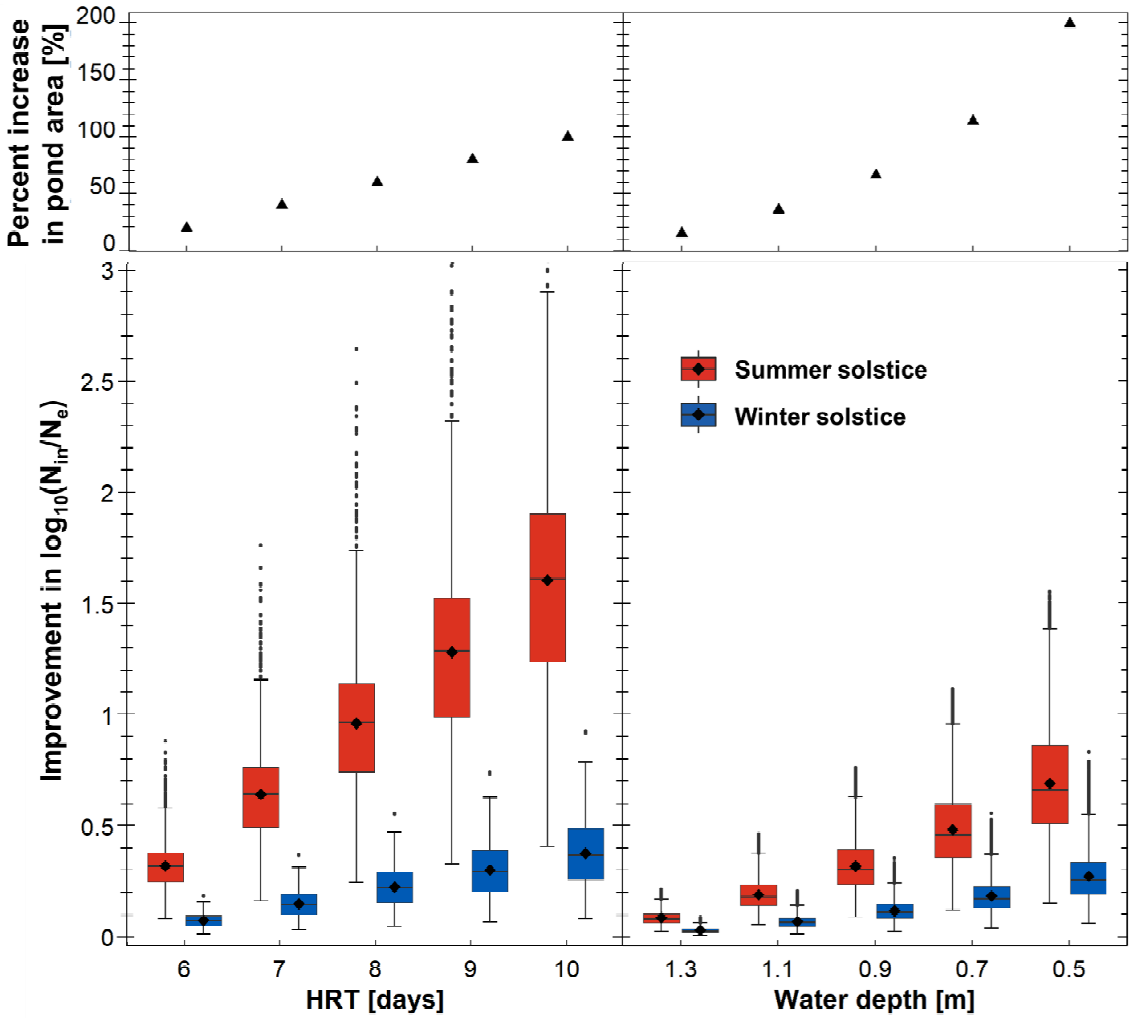

Figure 5. Simulated daily-average improvement in MS2 log inactivation of maturation pond system by increasing HRT or reducing pond depth compared to the baseline scenario (HRT = 5 days, depth = 1.5 m, configuration varies as described in detail in Fig S12), with corresponding percent increase in required pond area. Variations of the improvements in log inactivation were caused by the uncertainty in water quality and photo-reactivity parameters. Left: HRT was increased by adding ponds (HRT = 1 d) in series, and depth was fixed at 1.5 m; Right: depth was reduced with HRT fixed at 5 days, but configuration of the system varied. The box indicates 1st, 2nd and 3rd quartiles. The lower whisker shows the minimum, and the upper whisker = 3rd quartile + 1.5 × interquartile range.

Advancing sunlight inactivation modeling in natural and engineered systems. This work quantified the relative importance of different parameters to virus inactivation through global sensitivity analyses of a mechanistic sunlight virus inactivation model. Simultaneous variation of 14 parameters induced a considerable amount of variance in the prediction of k_{total} for all virus species and both water types. Investigation of "abnormal" cases in the simulations helped gain insight into how the important factors impact each inactivation mechanism.

Analysis results suggested that using MS2 as the single surrogate of sunlight virus inactivation may cause overestimation of the disinfection efficacy of a treatment system under certain conditions that suppress endogenous inactivation rates or enhance exogenous rates, most notably high NPOC concentration (> 30 mg-C·L^{-1} and low sunlight exposure around sunrise or sunset (zenith angle > 70°), because MS2 inactivation dominated by exogenous mechanism that is less sensitive to changes of sunlight exposure. The contribution of $^1O_2$ and ^{3}CDOM* to k_{exo} was strongly correlated with NPOC concentration in the water and significantly affected by water absorbance as well as concentrations of NO_3^- and NO_2^- for all viruses. When NPOC concentration is lower than 5 mg-C·L^{-1}, $^1O_2$ and ^{3}CDOM* together likely account for less than 50% of exogenous inactivation. Therefore, $^1O_2$ is not a valid surrogate for exogenous inactivation across the full range of physicochemical conditions of water.

Global sensitivity analyses showed a few environmental and design parameters significantly outweigh most water quality and virus photoreactivity parameters in determining virus inactivation rate constants. Diurnal motion of the sun is the most important single source of variability of k_{total}, followed by depth and NPOC concentration of the water column. However, seasonable solar motion was not as impactful as Φ_{virus}. Reducing the uncertainty in Φ_{virus} can most effectively improve the prediction accuracy of the sunlight inactivation model. If the variability of environmental, water quality or design parameters were not reduced, uncertainty in

$k_{virus,\ \cdot \mathrm{OH}}$, $k_{virus,\ \mathrm{CO}_3^{\cdot -}}$, and $k_{virus,{}^3\mathrm{CDOM}^*}$ would remain uninfluential to the prediction of k_{total} within the ranges evaluated. Since one cannot eliminate the variability in sunlight irradiance introduced by diurnal or seasonal solar motions and has little control over the variability of physiochemical conditions in influent waters, the evaluated uncertainty in $k_{virus,\ \cdot OH}$, $k_{virus,\ \mathrm{CO}_3^{\cdot -}}$, and $k_{virus,{}^3\mathrm{CDOM}^*}$ would remain relatively unimportant to the prediction of the inactivation efficacy.

Using an ideal CSTR model, this work estimated and compared the improvement in virus inactivation efficacy resulting from different design decisions of a hypothetical treatment system. Increasing HRT by adding maturation ponds in series was estimated to be the most cost-effective strategy in this model. However, one should be aware of the boundary and the assumptions of the model while attempting to apply the model to the prediction of the virus disinfection of an actual treatment system. The model in this study does not consider the variability or effects of pH, dissolved oxygen, or temperature in sunlight inactivation because they were shown to have insignificant inactivation effects within the relevant ranges[20,43,46] and thus had yet been explicitly incorporated in existing verified mechanistic aquatic photochemistry models. Microbial grazing of viruses was not considered but would likely differ across HRTs (longer HRT would allow for more grazing). Absorbance by algae and cyanobacteria in the wavelength range relevant for virus inactivation was assumed to be minimal compared to CDOM, and the water bodies were assumed well mixed without stratification. Parameter values for WSP were estimated based on a single WSP water. Therefore, results regarding WSP water may not be representative for all WSP water.

Moving forward in sunlight virus inactivation modeling, we suggest focusing effort to reduce the uncertainty in the prediction of endogenous inactivation resulted from Φ_{virus}. This can be approached by calibrating Φ_{virus} against commonly used sunlight irradiance models for the purpose of model integration. While damage to viral components in sunlight inactivation is

mainly caused by photochemical reactions, sunlight irradiation can also increase pathogen die-offs by rising water temperature, facilitating algal growth, and increasing DO and pH, which could become significant factors in solar disinfection of drinking water (SODIS).[4,17,19] Incorporating the synergies among different sunlight-mediated inactivation mechanisms into the mechanistic modeling of sunlight inactivation allows more extensive application in different treatment systems. Experiments with virus species relevant for public health in wider ranges of environmental and physiochemical conditions, especially in treatment systems relying on sunlight for low-cost disinfection, can offer better coverage of the entire ranges of variations of relevant parameters, which will improve prediction accuracy of the models.

Conflict of Interest Statement

The authors declare no competing financial interest.

Associated Content

Supporting Information Available

The Supporting Information is available free of charge on the ACS Publication website at DOI:

Additional detail on the integrated solar inactivation model; setup of the SMARTS program for simulation; description of parameters in the photochemical model; sampling procedures for sensitivity analyses; modeling of MS2 log10 removal of maturation ponds; additional statistical analysis results of simulated solar virus inactivation rate constants.

Acknowledgements

The authors would like to acknowledge financial support from the U.S. Environmental Protection Agency (EPA) for partial funding through grant RD83582201-0 for the first and second authors. The contents of this paper are solely the responsibility of the grantee and do not necessarily represent the official views of the EPA. Further, the EPA does not endorse the purchase of any commercial products or services mentioned in this publication.

References

(1) Love, D. C.; Silverman, A.; Nelson, K. L. Human Virus and Bacteriophage Inactivation in Clear Water by Simulated Sunlight Compared to Bacteriophage Inactivation at a Southern California Beach. *Environ. Sci. Technol.* **2010**, *44* (18), 6965–6970. https://doi.org/10.1021/es1001924.

(2) Boehm, A. B.; Yamahara, K. M.; Love, D. C.; Peterson, B. M.; Mcneill, K.; Nelson, K. L. Covariation and Photoinactivation of Traditional and Novel Indicator Organisms and Human Viruses at a Sewage-Impacted Marine Beach. *Environ. Sci. Technol.* **2009**, *43* (21), 8046–8052. https://doi.org/10.1021/es9015124.

(3) Kohn, T.; Nelson, K. L. Sunlight-Mediated Inactivation of MS2 Coliphage via Exogenous Singlet Oxygen Produced by Sensitizers in Natural Waters. *Environ. Sci. Technol.* **2007**, *41* (1), 192–197. https://doi.org/10.1021/es061716i.

(4) McGuigan, K. G.; Conroy, R. M.; Mosler, H. J.; du Preez, M.; Ubomba-Jaswa, E.; Fernandez-Ibañez, P. Solar Water Disinfection (SODIS): A Review from Bench-Top to Roof-Top. *J. Hazard. Mater.* **2012**, *235–236*, 29–46. https://doi.org/10.1016/j.jhazmat.2012.07.053.

(5) Curtis, T. P.; Mara, D. D.; Dixo, N. G. H.; Silva, S. A. Light Penetration in Waste Stabilization Ponds. *Water Res.* **1994**, *28* (5), 1030–1038.

(6) Victor, R.; Kotter, R.; O'Brien, G.; Mitropoulos, M.; Panayi, G. Wastewater Use in Agriculture. In *WHO Guidelines for the Safe Use of Wastewater, Excreta and Greywater*; World Health Organization: Geneva, 2006; Vol. II, pp 1–196.

(7) Silverman, A. I.; Nguyen, M. T.; Jasper, J. T.; Boehm, A. B.; Nelson, K. L. Sunlight Inactivation of Fecal Indicator Bacteria in Open-Water Unit Process Treatment Wetlands: Modeling Endogenous and Exogenous Inactivation Rates. *Environ. Sci. Technol.* **2015**,

49 (5), 2757–2766. https://doi.org/10.1021/es5049754.

(8) Noyola, A.; Padilla-Rivera, A.; Morgan-Sagastume, J. M.; Güereca, L. P.; Hernández-Padilla, F. Typology of Municipal Wastewater Treatment Technologies in Latin America. *Clean - Soil, Air, Water* **2012**, *40* (9), 926–932. https://doi.org/10.1002/clen.201100707.

(9) Verbyla, M.; von Sperling, M.; Maiga, Y. Waste Stabilization Ponds. *Global Water Pathogens Project. Part 4 Management of Risk from Excreta and Wastewater*. UNESCO 2017, pp 1–18.

(10) Verbyla, M. E.; Mihelcic, J. R. A Review of Virus Removal in Wastewater Treatment Pond Systems. *Water Res.* **2015**, *71* (860), 107–124. https://doi.org/10.1016/j.watres.2014.12.031.

(11) Nelson, K. L.; Boehm, A. B.; Davies-colley, R. J.; Dodd, M. C.; Kohn, T.; Linden, K. G.; Liu, Y.; Maraccini, P. A.; Mcneill, K.; Mitch, W. A.; et al. Sunlight-Mediated Inactivation of Health-Relevant Microorganisms in Water: A Review of Mechanisms and Modeling Approaches. *Environ. Sci. Process. Impacts* **2018**, *20* (8), 1089–1122. https://doi.org/10.1039/c8em00047f.

(12) Davies-Colley, R. J.; Donnison, A. M.; Speed, D. J.; Ross, C. M.; Nagels, J. W. Inactivation of Faecal Indicator Microorganisms in Waste Stabilisation Ponds: Interactions of Environmental Factors with Sunlight. *Water Res.* **1999**, *33* (5), 1220–1230.

(13) Kohn, T.; Grandbois, M.; Mcneill, K.; Nelson, K. L. Association with Natural Organic Matter Enhances the Sunlight-Mediated Inactivation of MS2 Coliphage by Singlet Oxygen. *Environ. Sci. Technol.* **2007**, *41* (13), 4626–4632. https://doi.org/10.1021/es070295h.

(14) Davies-Colley, R. J.; Donnison, A. M.; Speed, D. J. Towards a Mechanistic Understanding of Pond Disinfection. *Water Sci. Technol.* **2000**, *42* (10–11), 149–158.

(15) Sinton, L. W.; Hall, C. H.; Lynch, P. a; Davies-Colley, R. J. Sunlight Inactivation of Fecal Indicator Bacteria and Bacteriophages from Waste Stabilization Pond Effluent in Fresh and Saline Waters. *Appl. Environ. Microbiol.* **2002**, *68* (3), 1122–1131. https://doi.org/10.1128/AEM.68.3.1122.

(16) Romero-Maraccini, O. C.; Sadik, N. J.; Rosado-Lausell, S. L.; Pugh, C. R.; Niu, X. Z.; Croué, J. P.; Nguyen, T. H. Sunlight-Induced Inactivation of Human Wa and Porcine OSU Rotaviruses in the Presence of Exogenous Photosensitizers. *Environ. Sci. Technol.* **2013**, *47* (19), 11004–11012. https://doi.org/10.1021/es402285u.

(17) Romero, O. C.; Straub, A. P.; Kohn, T.; Nguyen, T. H. Role of Temperature and Suwannee River Natural Organic Matter on Inactivation Kinetics of Rotavirus and Bacteriophage MS2 by Solar Irradiation. *Environ. Sci. Technol.* **2011**, *45* (24), 10385–10393. https://doi.org/10.1021/es202067f.

(18) Rosado-Lausell, S. L.; Wang, H.; Gutiérrez, L.; Romero-Maraccini, O. C.; Niu, X. Z.; Gin, K. Y. H.; Croué, J. P.; Nguyen, T. H. Roles of Singlet Oxygen and Triplet Excited State of Dissolved Organic Matter Formed by Different Organic Matters in Bacteriophage MS2 Inactivation. *Water Res.* **2013**, *47* (14), 4869–4879. https://doi.org/10.1016/j.watres.2013.05.018.

(19) Carratalà, A.; Calado, A. D.; Mattle, M. J.; Meierhofer, R.; Luzi, S.; Kohn, T. Solar Disinfection of Viruses in Polyethylene Terephthalate Bottles. *Appl. Environ. Microbiol.* **2016**, *82* (1), 279–288. https://doi.org/10.1128/AEM.02897-15.

(20) Maiga, Y.; Wethe, J.; Denyigba, K.; Ouattara, A. S. The Impact of Pond Depth and Environmental Conditions on Sunlight Inactivation of Escherichia Coli and Enterococci in Wastewater in a Warm Climate. *Can. J. Microbiol.* **2009**, *55* (12), 1364–1374. https://doi.org/10.1139/W09-104.

(21) Silverman, A. I.; Peterson, B. M.; Boehm, A. B.; McNeill, K.; Nelson, K. L. Sunlight Inactivation of Human Viruses and Bacteriophages in Coastal Waters Containing Natural Photosensitizers. *Environ. Sci. Technol.* **2013**, *47* (4), 1870–1878. https://doi.org/10.1021/es3036913.

(22) Fisher, M. B.; Love, D. C.; Schuech, R.; Nelson, K. L. Simulated Sunlight Action Spectra for Inactivation of MS2 and PRD1 Bacteriophages in Clear Water. *Environ. Sci. Technol.* **2011**, *45* (21), 9249–9255. https://doi.org/10.1021/es201875x.

(23) Mattle, M. J.; Vione, D.; Kohn, T. Conceptual Model and Experimental Framework to Determine the Contributions of Direct and Indirect Photoreactions to the Solar Disinfection of MS2, PhiX174, and Adenovirus. *Environ. Sci. Technol.* **2015**, *49* (1), 334–342. https://doi.org/10.1021/es504764u.

(24) Kohn, T.; Mattle, M. J.; Minella, M.; Vione, D. A Modeling Approach to Estimate the Solar Disinfection of Viral Indicator Organisms in Waste Stabilization Ponds and Surface Waters. *Water Res.* **2016**, *88*, 912–922. https://doi.org/10.1016/j.watres.2015.11.022.

(25) Silverman, A. I.; Sedlak, D. L.; Nelson, K. L. Simplified Process to Determine Rate Constants for Sunlight-Mediated Removal of Trace Organic and Microbial Contaminants in Unit Process Open-Water Treatment Wetlands. *Environ. Eng. Sci.* **2019**, *36* (1), 43–59. https://doi.org/10.1089/ees.2018.0177.

(26) Nguyen, M. T.; Silverman, A. I.; Nelson, K. L. Sunlight Inactivation of Ms2 Coliphage in the Absence of Photosensitizers: Modeling the Endogenous Inactivation Rate Using a Photoaction Spectrum. *Environ. Sci. Technol.* **2014**, *48* (7), 3891–3898. https://doi.org/10.1021/es405323p.

(27) Silverman, A. I.; Tay, N.; Machairas, N. Comparison of Biological Weighting Functions Used to Model Endogenous Sunlight Inactivation Rates of MS2 Coliphage. *Water Res.*

2019, *151*, 439–446. https://doi.org/10.1016/j.watres.2018.12.015.

(28) Amarasiri, M.; Kitajima, M.; Nguyen, T. H.; Okabe, S. Bacteriophage Removal Efficiency as a Validation and Operational Monitoring Tool for Virus Reduction in Wastewater Reclamation : Review. *Water Res.* **2017**, *121*, 258–269. https://doi.org/10.1016/j.watres.2017.05.035.

(29) Bodrato, M.; Vione, D. APEX (Aqueous Photochemistry of Environmentally Occurring Xenobiotics): A Free Software Tool to Predict the Kinetics of Photochemical Processes in Surface Waters. *Environ. Sci. Process. Impacts* **2014**, *16* (4), 732–740. https://doi.org/10.1039/C3EM00541K.

(30) De Laurentiis, E.; Minella, M.; Bodrato, M.; Maurino, V.; Minero, C.; Vione, D. Modelling the Photochemical Generation Kinetics of 2-Methyl-4-Chlorophenol, an Intermediate of the Herbicide MCPA (2-Methyl-4-Chlorophenoxyacetic Acid) in Surface Waters. *Aquat. Ecosyst. Heal. Manag.* **2013**, *16* (2), 216–221. https://doi.org/10.1080/14634988.2013.788433.

(31) Marchetti, G.; Minella, M.; Maurino, V.; Minero, C.; Vione, D. Photochemical Transformation of Atrazine and Formation of Photointermediates under Conditions Relevant to Sunlit Surface Waters: Laboratory Measures and Modelling. *Water Res.* **2013**, *47* (16), 6211–6222. https://doi.org/10.1016/j.watres.2013.07.038.

(32) Maddigapu, P. R.; Minella, M.; Vione, D.; Maurino, V.; Minero, C. Modeling Phototransformation Reactions in Surface Water Bodies : 2, 4-Dichloro-6-Nitrophenol As a Case Study. *Environ. Sci. Technol.* **2011**, *45* (1), 209–214.

(33) Zepp, R. G.; Cline, D. M. Rates of Direct Photolysis in Aquatic Environment. *Environ. Sci. Technol.* **1977**, *11* (4), 359–366. https://doi.org/10.1021/es60127a013.

(34) Gueymard, C. A. Interdisciplinary Applications of a Versatile Spectral Solar Irradiance

Model: A Review. *Energy* **2005**, *30* (9 SPEC. ISS.), 1551–1576. https://doi.org/10.1016/j.energy.2004.04.032.

(35) Jarvis, A.; Reuter, H. I.; Nelson, A.; Guevara, E. Hole-filled SRTM for the globe Version 4 https://cgiarcsi.community/data/srtm-90m-digital-elevation-database-v4-1/ (accessed Mar 4, 2018).

(36) Vione, D.; Maurino, V.; Minero, C.; Carlotti, M. E.; Chiron, S.; Barbati, S. Modelling the Occurrence and Reactivity of the Carbonate Radical in Surface Freshwater. *Comptes Rendus Chim.* **2009**, *12* (8), 865–871. https://doi.org/10.1016/j.crci.2008.09.024.

(37) Vione, D.; Das, R.; Rubertelli, F.; Maurino, V.; Minero, C.; Barbati, S.; Chiron, S. Modelling the Occurrence and Reactivity of Hydroxyl Radicals in Surface Waters: Implications for the Fate of Selected Pesticides. *Int. J. Environ. Anal. Chem.* **2010**, *90* (3–6), 260–275. https://doi.org/10.1080/03067310902894218.

(38) De Laurentiis, E.; Minella, M.; Maurino, V.; Minero, C.; Brigante, M.; Mailhot, G.; Vione, D. Photochemical Production of Organic Matter Triplet States in Water Samples from Mountain Lakes, Located below or above the Tree Line. *Chemosphere* **2012**, *88* (10), 1208–1213. https://doi.org/10.1016/j.chemosphere.2012.03.071.

(39) Vione, D.; Lauri, V.; Minero, C.; Maurino, V.; Malandrino, M.; Carlotti, M. E.; Olariu, R. I.; Arsene, C. Photostability and Photolability of Dissolved Organic Matter upon Irradiation of Natural Water Samples under Simulated Sunlight. *Aquat. Sci.* **2009**, *71* (1), 34–45. https://doi.org/10.1007/s00027-008-8084-3.

(40) Mamane, H.; Shemer, H.; Linden, K. G. Inactivation of E. Coli, B. Subtilis Spores, and MS2, T4, and T7 Phage Using UV/H2O2 Advanced Oxidation. *J. Hazard. Mater.* **2007**, *146* (3), 479–486. https://doi.org/10.1016/j.jhazmat.2007.04.050.

(41) Mian, I. A.; Begum, S.; Riaz, M.; Ridealgh, M.; McClean, C. J.; Cresser, M. S. Spatial and

Temporal Trends in Nitrate Concentrations in the River Derwent, North Yorkshire, and Its Need for NVZ Status. *Sci. Total Environ.* **2010**, *408* (4), 702–712. https://doi.org/10.1016/j.scitotenv.2009.11.020.

(42) The Swiss Federal Council. *Waters Protection Ordinance*; 2014.

(43) Dias, D. F. C.; Passos, R. G.; von Sperling, M. A Review of Bacterial Indicator Disinfection Mechanisms in Waste Stabilisation Ponds. *Rev. Environ. Sci. Biotechnol.* **2017**, *16* (3), 517–539. https://doi.org/10.1007/s11157-017-9433-2.

(44) von Sperling, M. Volume 3: Waste Stabilisation Ponds. In *Biological Wastewater Treatment Series*; IWA, 2007; pp 1–162.

(45) Kayombo, S.; Mbwette, T. S. A.; Katima, J. H. Y.; Ladegaard, N.; Jørgensen, S. E. *Waste Stabilization Ponds and Constructed Wetlands: Design Manual*; 2005.

(46) Davies-Colley, R. J. Pond Disinfection. In *Pond Treatment Technology*; Shilton, A., Ed.; IWA Publishing: London, 2005; pp 100–136. https://doi.org/10.2166/9781780402499.

(47) Morris, M. D. Factorial Plans for Preliminary Computational Experiments. *Technometrics* **1991**, *33* (2), 161–174.

(48) Saltelli, A. Sensitivity Analysis for Importance Assessment. *Risk Anal.* **2002**, *22* (3), 579–590. https://doi.org/10.1002/0470870958.ch2.

(49) Campolongo, F.; Cariboni, J.; Saltelli, A. An Effective Screening Design for Sensitivity Analysis of Large Models. *Environ. Model. Softw.* **2007**, *22* (10), 1509–1518. https://doi.org/10.1016/j.envsoft.2006.10.004.

(50) Saltelli, A.; Tarantola, S.; Campolongo, F.; Ratt. *Sensitivity Analysis in Practice: A Guide to Assessing Scientific Models*; 2004. https://doi.org/10.1198/jasa.2006.s80.

(51) Saltelli, A.; Tarantola, S.; Campolongo, F.; Ratto, M. *Sensitivity Analysis in Practice: A*

Guide to Assessing Scientific Models; John Wiley & Sons Ltd: Chichester, 2004.

(52) Sobol', I. M. Sensitivity Analysis for Nonlinear Mathematical Models. *Math. Model. Comput. Exp.* **1993**, *1* (4), 407–414. https://doi.org/10.18287/0134-2452-2015-39-4-459-461.

(53) Iooss, B.; Lemaitre, P. A Review on Global Sensitivity Analysis Methods. In *Uncertainty Management in Simulation-Optimization of Complex Systems: Algorithms and Applications*; Meloni, C., Dellino, G., Eds.; Springer, 2015; pp 1–24.

(54) Herman, J.; Usher, W. SALib : An Open-Source Python Library for Sensitivity Analysis. *J. Open Source Softw.* **2017**, *41* (1), 9–10. https://doi.org/10.1016/S0010-1.

(55) Vione, D.; Minella, M.; Maurino, V.; Minero, C. Indirect Photochemistry in Sunlit Surface Waters: Photoinduced Production of Reactive Transient Species. *Chem. - A Eur. J.* **2014**, *20* (34), 10590–10606. https://doi.org/10.1002/chem.201400413.

(56) Boehm, A. B.; Silverman, A. I.; Schriewer, A.; Goodwin, K. Systematic Review and Meta-Analysis of Decay Rates of Waterborne Mammalian Viruses and Coliphages in Surface Waters. *Water Res.* **2019**, *164*, 114898. https://doi.org/10.1016/j.watres.2019.114898.